Two-dimensional low-coherence interferometry for the characterization of nanometer-wafer-topographies

Ch. Taudt[a,b,c], T. Baselt[a,c,d], B. Nelsen[a], H. Aßmann[e], A. Greiner[e], E. Koch[b] and P. Hartmann[a,c]

[a]University of Applied Sciences Zwickau, Dr. Friedrichs-Ring 2a, Zwickau, Germany

[b]Medizinische Fakultät Carl Gustav Carus, Technische Universität Dresden, Dresden, Germany

[c]Fraunhofer-Institut für Werkstoff- und Strahltechnik IWS, Dresden, Germany

[d]Fakultät für Maschinenwesen, Technische Universität Dresden, Dresden, Germany

[e]Infineon Technologies Dresden GmbH, Dresden, Germany

ABSTRACT

Within this work a scan-free, low-coherence inteferometry approach for surface profilometry with nm-precision is presented. The basic setup consist of a MICHELSON-type interferometer which is powered by a supercontinuum light-source ($\Delta\lambda = 400 - 1700\ nm$). The introduction of an element with known dispersion delivers a controlled phase variation which can be detected in the spectral domain and used to reconstruct height differences on a sample. In order to enable scan-free measurements, the interference signal is spectrally decomposed with a grating and imaged onto a two-dimensional detector. One dimension of this detector records spectral, and therefore height information, while the other dimension stores the spatial position of the corresponding height values.

In experiments on a height standard, it could be shown that the setup is capable of recording multiple height steps of 101 nm over a range of 500 μm with an accuracy of about 11.5 nm. Further experiements on conductive paths of a micro-electro-mechanical systems (MEMS) pressure sensor demonstrated that the approach is also suitable to precisely characterize nanometer-sized structures on production-relevant components. The main advantage of the proposed measurement approach is the possibility to collect precise height information over a line on a surface without the need for scanning. This feature makes it interesting for a production-accompanying metrology.

Keywords: optical metrology, interferometric measurement, dispersion based measurements, in-line characterization, low-coherence interferometry, surface profilometry

1. INTRODUCTION

Increased complexity and high production volumes in modern manufacturing of structures demand appropriate metrology and inspection methods, [1, 2]. Geometric deviations of structures and material inhomogenities can lead to systematic errors during all steps of manufacturing which might effect the quality and functionality of large volumes of a product. Especially in applications like power semiconductors [3], photovoltaics [4], defect detection in MEMS [5] as well as printied electronics [6, 7], production-accompanying metrology becomes vital. As feature size decreases dramatically and substrates get thinned in order to optimize performance, handling becomes delicate and small process variations, e.g. in positioning, can have huge influences on the manufacturing of important features. Most notably, unwanted deviations on parameters like the surface roughness and topography can cause major problems in processes such as lithography, [8]. In order to increase the yield and use all advantages of advanced manufacturing technologies, precise and process-accompanying metrology is required, [9]. The main demands for tools to measure surface features are nm-axial resolution, μm-lateral resolution and the possibility to perform measurements on production structures during the manufacturing. One key aspect

Further author information: (Send correspondence to Ch. Taudt)
Ch. Taudt, e-mail: christopher.taudt@fh-zwickau.de, Telephone: +49 375 536 1972
P. Hartmann, e-mail: peter.hartmann@fh-zwickau.de, Telephone: +49 375 536 1538

in the characterization of production materials, in opposition to test samples, is the possibility to measure on a wide range of materials and surface compositions. The characterization of multiple layered material structures and high aspect ratios are especially demanding for existing metrology.
Tools like atomic force microscopy (AFM) perform well in terms of axial and lateral resolution, [10]. They have been shown to be excellent tools in laboratory environments for applications such as microbiology and nano-structured materials [11–13]. However, AFM measurements over areas larger than the standard (5 x 5 μm) require special installations and measurement times increase significantly, [14].
A second common measurement technology in the semiconductor industry is so called scatterometry which retrieves surface profile information based on reflected intensities, [15–17]. The technique relies on the reflection on periodic surface structures where a well-known model of the materials and the structures involved enable nm-precise measurements, [18,19]. These requirements limit its flexibility and the use as an in-line tool. Furthermore, metrology approaches such as confocal laser scanning microscopy [20] and scanning white-light interferometry [21] have shown the appropriate accuracy. Though these technologies deliver a good performance on a lab scale with appropriate test samples, they are not applicable to situations in a production environment with more complex samples due to speed issues, [22].
Within this work, an alternative approach based on low-coherence interferometry is proposed, implemented and tested. This approach aims to be both precise in the nm-range regarding surface profiles, and adaptable to be integrated into a production machine or line.

2. EXPERIMENTAL APPROACH

A modified low-coherence interferometer is combined with an imaging spectrometer in order to perform nm-precise, scan-free height profilometry. For that purpose, the interferometer is powered by a supercontinuum light source ($\Delta\lambda = 400 - 1700\ nm$, ilum 1, Fiberware GmbH, Germany), Fig. 1. In this configuration the reference

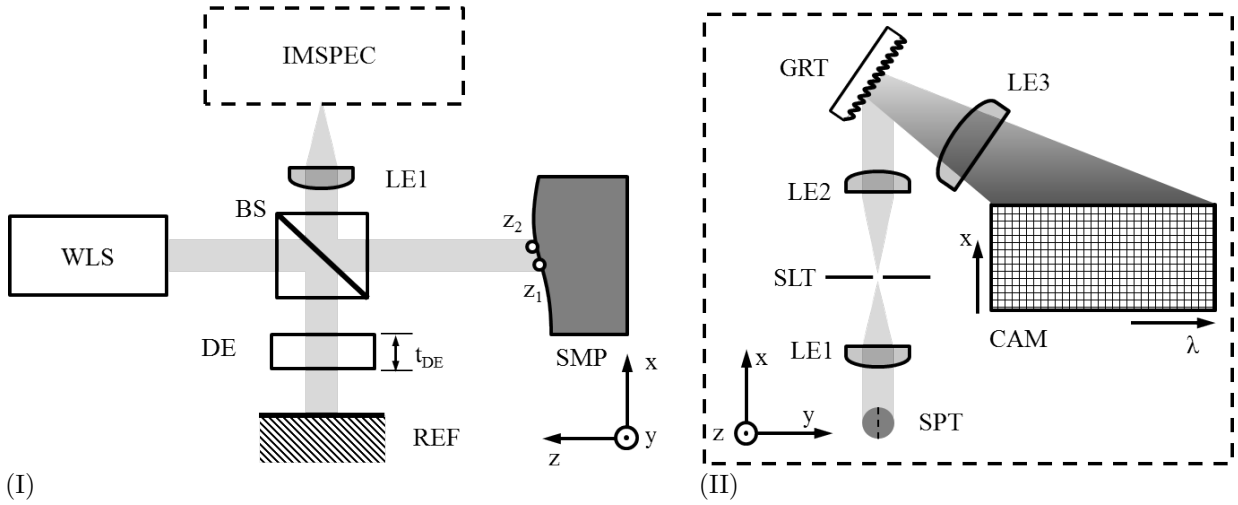

Figure 1. (I) Experimental setup with WLS - white-light source, BS - beam splitter, SMP - sample where z_1 and z_2 are two different heights, REF - fixed reference mirror, DE - dispersive element with the thickness t_{DE}, LE1 - lens to image the sample onto the spectrometer, IMSPEC - imaging spectrometer and a detailed view of the same in (II) with SPT - measurement spot, SLT - slit, LE2 - collimating lens, GRT - grating, LE3 - imaging lens and CAM - camera where the spectral information for every point on the line in x-dimension is recorded

arm is composed of an element with known dispersion (here Schott N-BK7, $t_{DE} = 2000\ \mu m$) and a plain mirror. The sample arm holds a sample with a varying height profile along the x-y plane noted with $z(x, y)$. The recombined collimated light from sample and reference arms is imaged on the slit of an imaging spectrometer. Within this spectrometer the light is spectrally decomposed and imagaged onto the two-dimensional CMOS array of a camera. In difference to a single-line detector in a standard spectrometer, this configuration enables the detection of spectra at every point on a line in the x-dimension of the measurement spot. The information

is only selected from one point in the y-direction which means that the acquisition of single-shot height profiles along a single line at once becomes possible.
The output signal from the spectrometer can be described by using common two-beam interferometer equations [23] under the consideration of the dispersion in the system [24]:

$$I(\lambda, x) = I_0(\lambda) \cdot (1 + \cos \phi(\lambda, x)) \tag{1}$$

$$\phi(\lambda, x) = 2\pi \frac{(n(\lambda) - 1)t_{DE} - \delta(x)}{\lambda} \tag{2}$$

where $I_0(\lambda)$ is the initial spectral intensity before the beam splitter and $\phi(\lambda, x)$ is the absolute phase of the signal at every point in the x-dimension which is dependent on the optical path difference (OPD) between both arms denoted with $\delta(x)$ and the wavelength λ. The introduced dispersion due to the wavelength dependent refractive index $n(\lambda)$ and the material's thickness t_{DE} transforms the initial interference signal. The periodicity of fringes tends to a minimum, when the so called equalization wavelength λ_{eq}, which is dependent of the OPD, is reached, Fig. 2.
When using the interferometer as a profilometer, every height change in the sample's surfaces (e.g. z_1, z_2 and z_n)

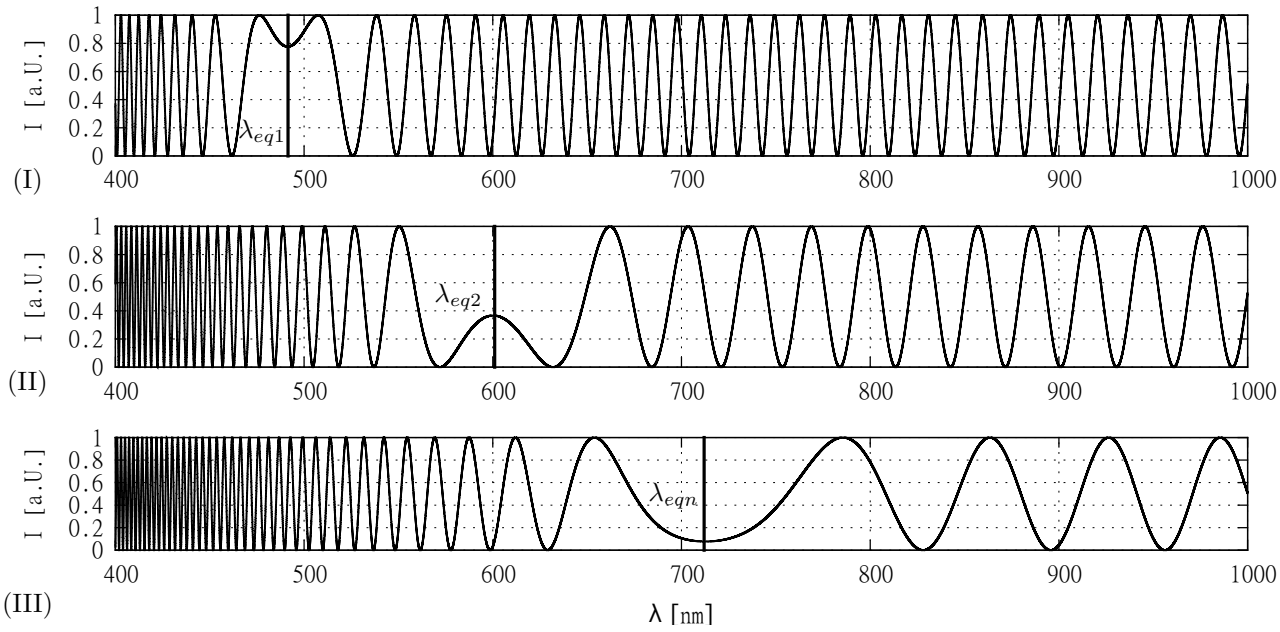

Figure 2. Schematic representation of intensity signals on different points in the x-dimension (I-III) where the samples surface with independent heights (e.g. z_1, z_2 and z_n) leads to different equalization wavelengths λ_{eq1}, λ_{eq2} and λ_{eqn}

along the x-dimension changes the path length $\delta(x)$. This therefore leads to different spectra for every position on the sample in the x-dimension with corresponding equalization wavelengths (e.g. λ_{eq1}, λ_{eq2} and λ_{eqn}). A curve fit and the determination of the equalization wavelength can be done using the data gathered with the spectrometer, [25]. The equalization wavelength can be found by calculating the zero of the derivative of the phase signal:

$$\left(\frac{\partial \phi}{\partial \lambda}\right)_{\lambda_{eq}} = 0 \tag{3}$$

The relative or absolute height $z(x)$ at a given point in the x-dimension can be calculated by fitting the corresponding, recorded spectrum and determining the equalization wavelength which will lead to a certain path length $\delta(x)$. The choice of the dispersive element determines the measurement range Δz:

$$\Delta z(\lambda) = n_{group}(\lambda) \cdot \frac{t_{DE}}{2} \tag{4}$$

where $n_{group}(\lambda)$ is the group refractive index of the element's material. Furthermore, the dispersive element in combination with the spectral range of the light source, the spectrometer and the quality of the fitting routine determines the axial resolution.

3. RESULTS

Before performing all experiments, the imaging spectrometer was calibrated spectrally as well as spatially. The spectral calibration was carried out by fitting the line spectrum of gas-discharge lamp which was prevoiusly recorded with a calibrated spectrometer. In addition to that, the imaging spectrometer was calibrated in the spatial dimension of the camera chip by using a graduation test target (G391122000, Qioptiq Photonics GmbH & Co. KG, Germany) for the correct measurement of spatial information. The lateral resolution was found to be 1.94 μm in the used setup.
In order to evaluate the resolution of the above described setup, two sets of experiments have been carried out. In the first experiment the structure of a height standard was measured, while in the second experiment the height profile of a conductive path on a MEMS pressure sensor was characterized.
A silicon substrate with a series of steps having a nominal height of 101 nm in a 250 μm pitch served as a height standard (Simetrics VS, Simetrics GmbH, Germany). The standard was previously calibrated against a PTB standard 2002-0004. An initial equalization wavelength of 520 nm was adjusted for the first measurement on the top of the structure. In all following measurements, the equalization wavelength was determined by a least-squares fit procedure following equations (1)-(3). The surface profile was then calculated relative to the highest point, Fig. 3. The data was collected in ten consecutive measurements and is displayed averaged with

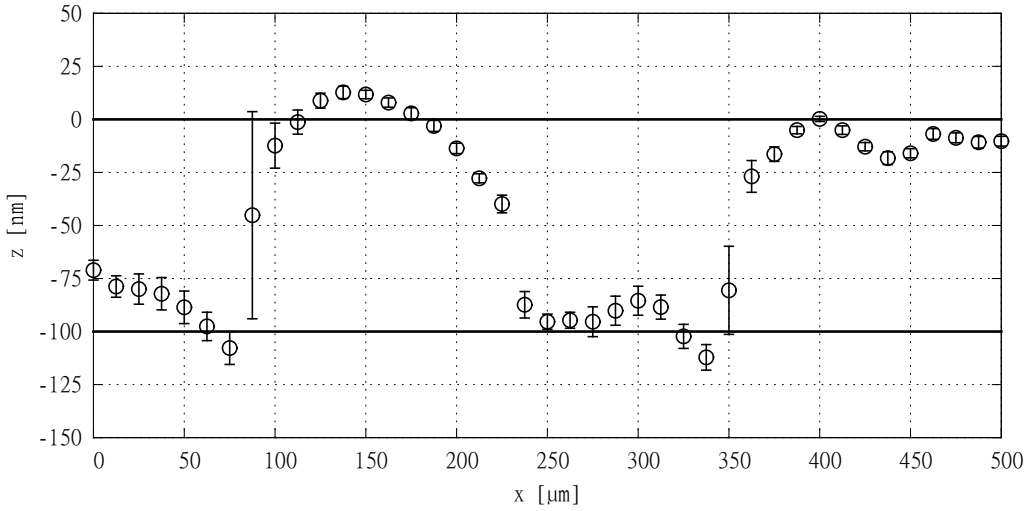

Figure 3. Results of the first experiment with measured line profile of the step height standard with a nominal height of $z_{nom} = 101$ nm where the errorbars represent the deviation from 10 consecutive measurements

the errorbars representing the repeatability of the measurements. The results were corrected accordingly to a minor tilt of the complete sample. It can be seen that the low-coherence interferometer is capable of a precise representation of the multiple step heights over a range of 500 μm. The mean step height measured was $\bar{z} = 103.4$ nm while the standard deviation was $z_\sigma = 1.4$ nm. In comparision to the nominal height of 101 nm the RMS error was calculated with $z_\epsilon = 11.5$ nm. This value points to a good agreement with the given confidence band of $\pm$ 10 nm given by the standard's manufacturer. The data also makes it obvious that the occurence of sharp edges on the sample influence the measurement negatively. Data points close to the sharp edges (compare data points in a distance e.g. 80 - 100 μm in Fig. 3) show significantly greater deviations from the nominal value. This leads to blurred edges stretching over a range of 20 μm where the edge should have risen a distance in the nm-range according to the manufacturer. Furthermore, the flatness of the respective sections is distorted while the error of consecutive measurements is highest in the areas of the edges. These edge effects might occure due

to scattering effects and the low numerical aperture of the optical setup which decrease the signal-to-noise ratio such that the fitting algorithms performance decreases as well.
As a second measurement, the surface structure of a MEMS pressure sensor was evaluated. These sensors typically consist out of membrane manufactured by etching a groove of desired depth in silicon. On the top of the membrane, resistors form a Wheatstone bridge where the deflection is electrically recorded by conductive paths which are bonded to external structures, Fig. 4 (I). The characterization of the height profile of one of these conductive paths with the height z_{ps} was the subject of the second experiment.
The measurements with the low-coherence interferometer were conducted in a comparable manner to the first experiment. An initial equalization wavelength of 520 nm was adjusted for the flat part of the chip. All data taken within this measurement were fitted using the above-mentioned algorithm. Afterwards, the surface profile was calculated relative to the initial level, Fig. 4 (II).
The data shows that the conductive path on the surface of the pressure sensor has a mean height of 79.6 nm

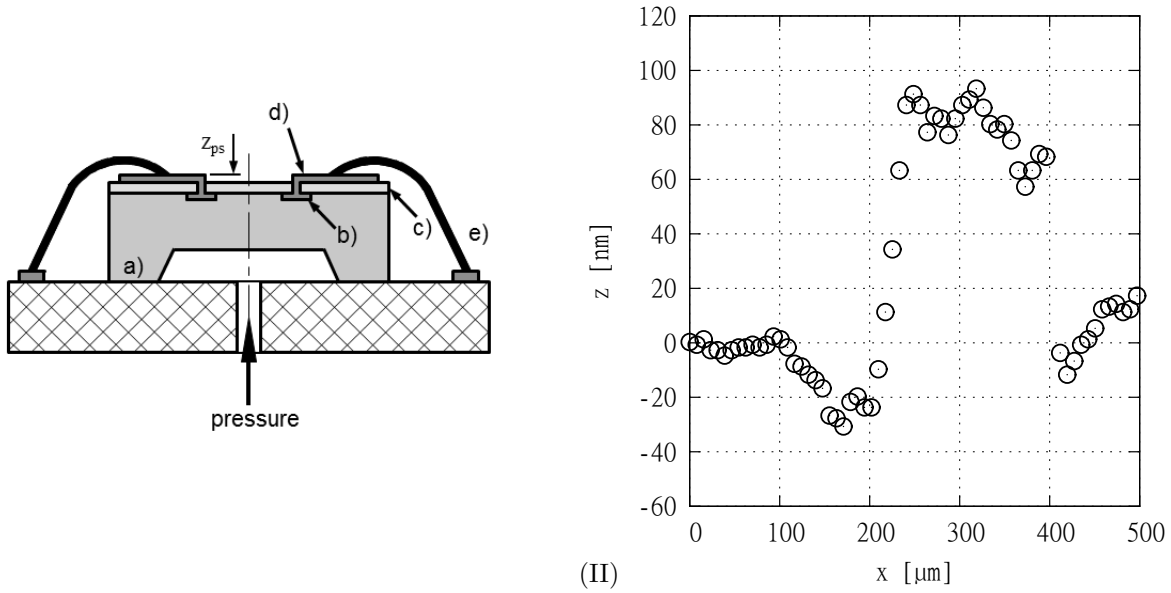

(I) (II)

Figure 4. (I) Cross-section of a MEMS pressure sensor with a) silicon pressure sensor body, b) resistors forming a Wheatstone bridge, c) passivation layer, d) conductive path with the height to be measured z_{ps}, e) bond wire an (II) Results of the second experiment with the height of the conductive path z_{ps} along the x-dimension

with a standard deviation of 9.4 nm and stretches over a width of 200 μm. The results show, as already seen in the first experiments, stronger deviations on the edges. It is visible that these deviations are effecting the measured flatness of the respective areas as well as sharpness of the edge representation.

4. CONCLUSION AND OUTLOOK

Within this work, a scan-free approach to low-coherence interferometry with nm-resolution in the height dimension of surface structres was presented. The setup consisted of an interferometer with known dispersion and broadband illumination where the interference signal was recorded on an imaging spectrometer with a two-dimensional detector. This enabled the recording of height information, encoded in the spectral data, over a line in a spatial dimension without the need for mechanical scanning.
Experiments on a silicon surface height standard showed that the system can resolve steps of 101 nm with an accuracy of 11.5 nm over range of 500 μm. The results showed some scattering effects in the areas of sharp edges of the standard's surface profile. This led to some error of the values close to the edge and a slightly blurred edge

representation. This source of error, as well as chromatic aberrations and uncertainties in the fitting routine, are subject to further developments to improve the system. The obtained results have shown that the desired accuracy is achievable with this approach so that measurements could be performed on relevant semiconductor structures.
For that purpose, the conductive paths of a Wheatstone bridge on the surface of a MEMS pressure sensor were investigated using this setup. It was clear from the reuslts that this structure had a height of 79.6 nm with a width of about 200 μm. Similarly, the results showed higher deviations in the sections with steep changes of the height profile. Due to the rather large measurement range in the in-plane direction of the pressure sensor and the high resolution in the height dimension, the approach might be suitable to record the deflection of the sensor under pressure with a necessary high resolution due to small pressure changes.
Further development will be done to improve the mechanical and temperature stability of the setup. The analyzing algorithm, as well as the computer hardware, also show room for improvement regarding speed and reliability. A major emphasis will be placed on the investigation and minimization of the edge effects by customizing the fitting algorithm as well as the optical setup for that purpose.
In comparison to other technologies where mechanical scanning is needed, the low-coherence interferometer approach enables faster measurements. This advantage makes it suitable for in-line measurements during the production of nm-scaled structures.

ACKNOWLEDGMENTS

This work is done as part of the project *eRamp*, which is co-funded by grants from ENIAC Joint Undertaking and from Germany, Austria, the Netherlands, Romania, Slovakia and the UK. Financial support by the German Federal Government (in particular from Bundesministerium für Bildung und Forschung) under Grant Nr. *16ES0233* is gratefully acknowledged. The authors want to additionally thank the members of the optical technologies working group at the West Saxon University of Applied Sciences Zwickau for fruitful discussions as well as the MEMS working group for providing the pressure sensor samples investigated within this work.

REFERENCES

[1] Leach, R., [*Optical measurement of surface topography*], Springer Berlin-Heidelberg, 1st ed. (2011).
[2] Osten, W. and Reingand, N., [*Optical Imaging and Metrology*], Wiley-VCH Verlag GmbH and Co. KGaA (2012).
[3] Wagner, R., "The transition of power semiconductor to 300mm." Semicon Europa Talk (2012).
[4] Kurtz, S., Wohlgemuth, J., Sample, T., Yamamichi, M., Amano, J., Hacke, P., Kempe, M., Kondo, M., Doi, T., and Otani, K., "Ensuring quality of pv modules," in [*Photovoltaic Specialists Conference (PVSC), 2011 37th IEEE*], 000842–000847 (June 2011).
[5] Shankar, N. G. and Zhong, Z. W., "Defect detection on semiconductor wafer surfaces," *Microelectron. Eng.* **77**, 337–346 (Apr. 2005).
[6] Group, O.-A., "Roadmap for organic and printed electronics 4th edn." Frankfurt: Organic and Printed. Electronics Association (2013).
[7] Caglar, U., *Studies of Inkjet Printing Technology with Focus on Electronic Materials*, PhD thesis, Tampere University of Technology (2010).
[8] Deboy, G. and Aigner, K., "Power semiconductors on 300-millimeter wafers," *Power Electronics Europe* **3**, 44–47 (2013).
[9] Pfitzner, L., Anger, S., Koitzsch, M., Schoepka, U., Roeder, G., Tobisch, A., Schellenberger, M., and Pfeffer, M., "Frontiers in defect detection," *Frontiers of Characterization and Metrology for Nanoelectronics* (2013).
[10] Guilhalmenc, C., Moriceau, H., Aspar, B., Auberton-Hervé, A., and Lamure, J., "Characterization by atomic force microscopy of the {SOI} layer topography in low-dose {SIMOX} materials," *Materials Science and Engineering: B* **46**(1 - 3), 29 – 32 (1997). E-MRS 1996 Spring Meeting, Symposium A: High Temperature Electronics: Materials, Devices and Applications.
[11] Giessibl, F. J., "Advances in atomic force microscopy," *Rev. Mod. Phys.* **75**, 949–983 (Jul 2003).

[12] Catena, A., McJunkin, T., Agnello, S., Gelardi, F. M., Wehner, S., and Fischer, C. B., "Surface morphology and grain analysis of successively industrially grown amorphous hydrogenated carbon films (a-c:h) on silicon," *Applied Surface Science* **347**, 657 – 667 (2015).

[13] Caglar, O., Carroy, P., Losio, P., and Sinicco, I., "Nanocrystalline zinc oxide for surface morphology control in thin-film silicon solar cells," *Solar Energy Materials and Solar Cells* **144**, 55 – 62 (2016).

[14] Lonardo, P., Lucca, D., and Chiffre, L. D., "Emerging trends in surface metrology," *CIRP Annals - Manufacturing Technolog* **51**, 701–723 (2002).

[15] Ku, Y.-S., Wang, S.-C., Shyu, D.-M., and Smith, N., "Scatterometry-based metrology with feature region signatures matching," *Opt. Express* **14**, 8482–8491 (Sep 2006).

[16] Drège, E. M., Reed, J. A., and Byrne, D. M., "Linearized inversion of scatterometric data to obtain surface profile information," *Opt. Eng.* **41**, 225–236 (2002).

[17] Tay, C. J. and Quan, C., "A parametric study on surface roughness evaluation of semi-conductor wafers by laser scattering," *International Journal for Light and Electron Optics* **114**, 1–6 (2003).

[18] Huang, H.-T. and Jr, F. L. T., "Spectroscopic ellipsometry and reflectometry from gratings (scatterometry) for critical dimension measurement and in situ, real-time process monitoring," *Thin Solid Films* **455–456**, 828 – 836 (2004). The 3rd International Conference on Spectroscopic Ellipsometry.

[19] Liu, S., Chen, X., and Zhang, C., "Development of a broadband mueller matrix ellipsometer as a powerful tool for nanostructure metrology," *Thin Solid Films* **584**, 176 – 185 (2015). The 7th International Conference on Technological Advances of Thin Films and Surface Coatings (ThinFilms2014).

[20] Udupa, G., Singaperumal, M., Sirohi, R. S., and Kothiyal, M. P., "Characterization of surface topography by confocal microscopy: I. principles and the measurement system," *Measurement Science and Technology* **11**(3), 305 (2000).

[21] Bowe, B. and Toal, V., "White light interferometric surface profiler," *Optical Engineering* **37**(6), 1796–1799 (1998).

[22] Leach, R., Evans, C., He, L., Davies, A., Duparré, A., Henning, A., Jones, C. W., and O'Connor, D., "Open questions in surface topography measurement: a roadmap," *Surface Topography: Metrology and Properties* **3**(1), 013001 (2015).

[23] Born, M. and Wolf, E., [*Principles of Optics: Electromagnetic Theory of Propagation, Interference and Diffraction of Light*], Cambridge University Press, 7th ed. (1999).

[24] Delbarre, H., Przygodzki, C., Tassou, M., and Boucher, D., "High-precision index measurement in anisotropic crystals using white-light spectral interferometry," *Applied Physics B* **70**(1), 45–51 (2000).

[25] Taudt, C., Augenstein, A., Baselt, T., Assmann, H., Greiner, A., Koch, E., and Hartmann, P., "Characterization of a dispersion-controlled approach to surface profilometry on wafers using a white-light interferometer," *Proc. SPIE* **9517**, 95170W–95170W–6 (2015).